Forsch Ingenieurwes (2021) 85:219–227
https://doi.org/10.1007/s10010-021-00459-w

ORIGINALARBEITEN/ORIGINALS

# Simulative investigation of ring creep on a planetary bearing of a wind turbine gearbox

Jonas Gnauert[1] · Felix Schlüter[1] · Georg Jacobs[1] · Dennis Bosse[1] · Stefan Witter[1]

Received: 16 December 2020 / Accepted: 4 March 2021 / Published online: 30 March 2021


**Abstract**
Wind turbines (WT) must be further optimized concerning availability and reliability. One of the major reasons of WT downtime is the failure of gearbox bearings. Some of these failures occur, due to the ring creep phenomenon, which is mostly detected in the planetary bearings. The ring creep phenomenon describes a relative movement of the outer ring to the planetary gear. In order to improve the understanding of ring creep, the finite element method (FEM) is used to simulate ring creep in planetary gears. First, a sensitivity analysis is carried out on a small bearing size (NU205), to characterize relevant influence parameters for ring creep—considered parameters are teeth module, coefficient of friction, interference fit and normal tooth forces. Secondly, a full-scale planetary bearing (SL185030) of a 1MW WT is simulated and verified with experimental data.

## Simulative Untersuchung des Ringwanderns an einem Planetenlager eines Planetengetriebes einer Windenergieanlage

**Zusammenfassung**
Windenergieanlagen (WEA) müssen hinsichtlich Verfügbarkeit und Zuverlässigkeit weiter optimiert werden. Einer der Hauptgründe für WEA-Ausfälle ist der Ausfall von Getriebelagern. Einige dieser Ausfälle treten aufgrund von Ringwandern auf, welches meist in den Planetenlagern zu beobachten ist. Das Ringwandern beschreibt eine Relativbewegung des Außenrings zum Planetenrad. Um das Verständnis des Ringwanderns zu verbessern, wird die Finite-Elemente-Methode (FEM) zur Simulation des Ringwanderns in Planetengetrieben eingesetzt. Zunächst wird eine Sensitivitätsanalyse an einer kleinen Lagergröße (NU205) durchgeführt, um relevante Einflussparameter für das Ringkriechen zu charakterisieren - die berücksichtigten Parameter sind Zahnmodul, Reibungskoeffizient, Presssitz und Zahnnormalkräfte. Zweitens wird ein maßstabsgerechtes Planetenlager (SL185030) einer 1-MW-Anlage simuliert und mit experimentellen Daten verifiziert.

## 1 Introduction

The wind industry is a major pillar of climate-friendly energy supply in Germany. The wind industry supplies 17.2% of the energy production, which sums up to 49.2% of the renewable resources [1]. To achieve a fully climate-friendly energy supply in Germany, it is important to ensure that the wind industry continues its growth and becomes even more competitive to fossil and nuclear sources. For this purpose, the levelized cost of energy generated by wind turbines (WT) must be reduced. Therefore, WT must be further optimized concerning availability and reliability. One of the major reasons of WT downtime is the failure of gearbox bearings. Significant amounts of these failures occur, due to the ring creep phenomenon, which is mostly detected in the planetary bearings. The absolute amount cannot be quantified further as ring creep itself does not cause a gearbox failure, but rather is the cause of secondary failure modes. As a consequence of ring creep, fretting corrosion and abrasive wear can occur in the bearing seat as well as on retaining rings and bearing flanges resulting in particles [11–14], which can lead to consequential damages to bearings and gear teeth [18]. As wear progresses, bearing

✉ Jonas Gnauert
Jonas.gnauert@cwd.rwth-aachen.de

[1] Chair for Wind Power Drives, RWTH Aachen, Campus-Boulevard 61, 52074 Aachen, Germany

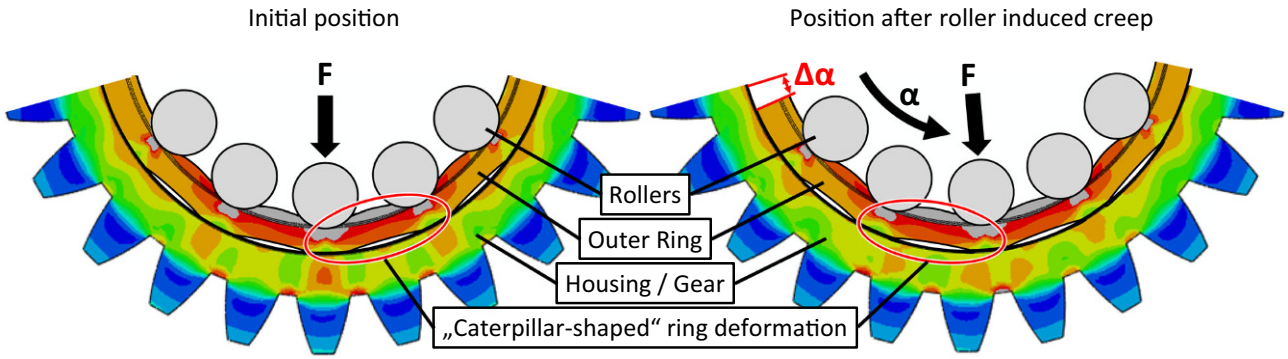


**Fig. 1** Schematic model of roller-induced ring creep and the "caterpillar-shaped" deformation (exaggerated) of the bearing ring [5]

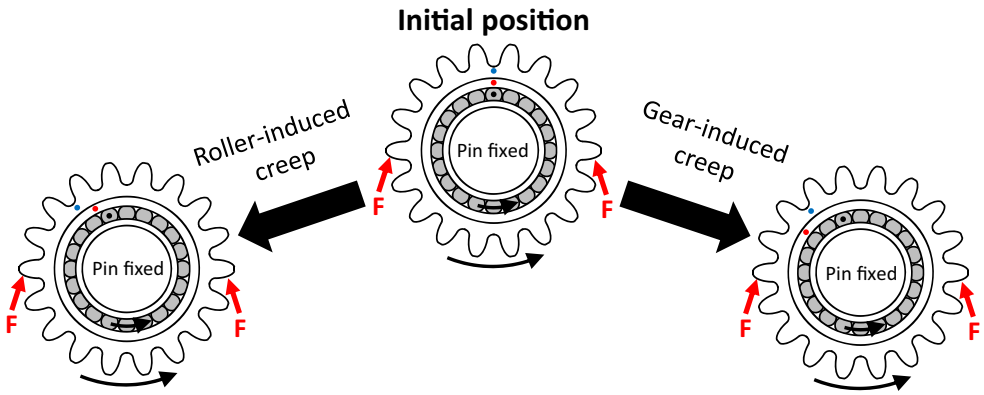


**Fig. 2** Rotational direction of the bearing ring (*red dot*) relative to the gear wheel (*blue dot*) for roller-induced creep (*left*) and gear-induced creep (*right*), after [5]

flanges [15] and retaining rings can break [16] in addition the progressive wear results in misalignments in the gear [11, 12, 14, 17, 18], which can lead to further damage to the gears [18].

Many simulative and experimental investigations were carried out regarding the ring creep phenomenon on small-scale model test benches [8] and ring creep is therefore well understood within the investigated parameter range. However, non-uniform gear load distribution as well as multiple-row bearing concepts, as commonly used in WT planetary gears, have been identified as highly relevant influences on ring creep [8], but until now, simulations could not be validated for a full-size wind turbine planetary bearing under realistic load conditions. Therefore, for the first time a validation of a ring creep simulation for a full-size wind turbine planetary bearing is presented in this paper, which is based on the experimental results of [2–4].

## 2 State of the art

The ring creep phenomenon describes a relative movement between the outer ring and the planetary gear. The relative movement is caused by local deformations, which result in locally high shear stresses that overcome the static friction and as a result local slip occurs in the bearing seat. Ring creep can be observed in tangential and axial direction. The focus of this investigation will be on tangential ring creep—also referred to as just ring creep. Ring creep has to be separated into two different types of ring creep: roller-induced and the gear-induced ring creep.

Roller-induced ring creep is caused by a "caterpillar-shaped" deformation of the bearing ring due to the concentrated forces of the rollers (see Fig. 1). Through this deformation, the compression of the interference fit is reduced between the rollers and can be overcome locally by tangential strain, which is caused by the moving rollers. Hence, local slip can occurs, which leads to a very small movement of the bearing ring relative to the gear with every overroll [7].

On the other hand gear-induced ring creep is caused by a deformation of the gear, through the bending of the tooth due to the normal tooth forces. Through this deformation, the compression of the interference fit is reduced behind each gear tooth engagement and can be overcome locally by tangential strain, which is caused by the rotation of the gear engagement. Thus, local slip can occur, which leads to a very small movement of the bearing ring relative to the gear. The direction of gear-induced ring creep is opposite to roller-induced ring creep (see Fig. 2) and can therefore even reverse under certain circumstances the resulting ring creep direction [4, 5, 7].

Simulation of ring creep has already been successfully performed several times using the finite element method, aiming the identification of geometric and constructive measures against ring creep [6–9]. The results of the simulations and experiments of [6–8] show good consistence and some factors have been identified that increase or decrease ring creep. For Example increasing nominal tooth forces, loose fits, thin bearing rings amplify while higher bearing clearance, wider bearing rings, more rollers and increased friction in the bearing seat weaken ring creep [8]. An advantage of simulations over experiments is the opportunity to create a better understanding of the system due to the possibility to observe the exact processes in the assembly. For example, it could be confirmed that the creep is caused by local slippage zones, which are triggered by shear stresses that can exceed the frictional engagement in the bearing seat. Those local slippage zones spread out over time as a result of the operating loads and finally reach the entire bearing seat [6]. However, until now only simulations of bearings that are significantly smaller than bearings used in WT gearboxes could be validated [8], so that the results cannot easily be transferred to planetary gears in WTs with non-uniform gear load distribution as well as multiple-row bearing concepts. The number of roller rows in a bearing or bearing arrangement influences the load distribution over the width of the bearing or bearing arrangement. This load distribution then determines the pressure distribution in the bearing seat which finally influences the creep behavior of the bearing ring at this position. Furthermore [4, 5, 8, 10] showed that non-uniform gear load distributions have a significant influence on ring creep, and in [10] it was only investigated experimentally.

## 3 Approach

In order to improve the understanding of ring creep, the finite element method (FEM) is used to simulate ring creep in planetary gears. First, a sensitivity analysis is carried out on a small bearing size (NU205), to characterize relevant influence parameters for ring creep—considered parameters are teeth module, coefficient of friction, interference fit and normal tooth forces. Secondly, a full-scale planetary bearing (SL185030) of a 1 MW WT is simulated and verified with experimental data [2–4, 10].

The FE models are created regarding to FVA-No. 479 VI [8], the models consist of an elastic planetary gear and bearing outer ring as well as several rigid rolling elements (see Fig. 3). The planetary gear stands still while the rolling elements and the normal tooth forces rotate.

The normal tooth forces are applied on the planetary gear along the planes of action, which also supports the use of non-uniform load profiles. The contact between the individual components is simulated as a hard contact and is frictionless for the rolling elements, which allows neglecting the rotation of the rolling element itself [6]. Between the bearing outer ring and the planetary gear, the tangential and axial hard contact is modelled with friction and an interference fit is implemented. The elasticity of the rolling element and the bearing inner ring is replicated by springs fixed at a center point.

## 4 Sensitivity analysis

The sensitivity analysis is carried out on a small bearing size (NU205), to characterize relevant influence parameters for ring creep—considered parameters are teeth module, coefficient of friction, interference fit and normal tooth forces. Each parameter was varied from a reference value. The parameters for the reference simulation and the variation of each parameter are listed in Table 1. The sensitivity analysis is carried out on a small size bearing to significantly reduce the computational effort, which on the other hand comes with some downs e.g. the tooth modulus and the number of teeth cannot be set to typical values for a planetary gear in WT. All simulations are carried out with a helix angle of 8° and a fixed number of teeth of 24 at the planetary gear. Through the fixed number of teeth, a change in teeth module also results in a change of the gear hub thickness (relative ring thicknesses are 1.41, 2.2 and 2.87).

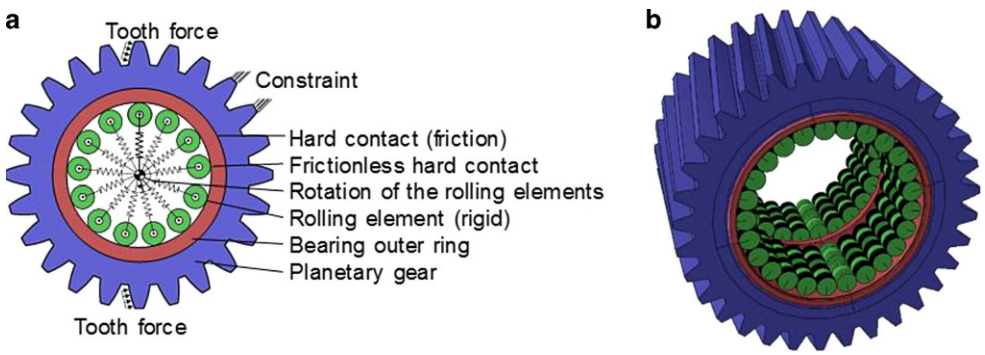


**Fig. 3** Structure of the finite element model to predict ring creep (**a**); Modell of the full-scale WT planetary bearing (**b**)

**Table 1** Parameters for the reference simulation and the variation of each parameter

| Parameter | Teeth module | Coefficient of friction | Interference fit | Normal tooth forces |
|---|---|---|---|---|
| Variation + | 3.25 mm | 0.4 | 25 µm | 25 kN |
| Reference | 3.00 mm | 0.3 | 20 µm | 20 kN |
| Variation – | 2.75 mm | 0.2 | 15 µm | 15 kN |

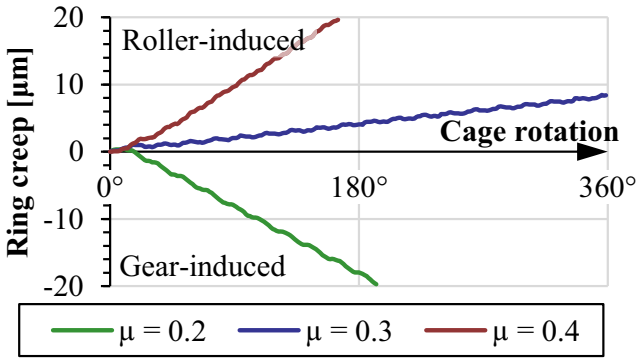


**Fig. 4** Ring creep [µm] per cage rotation depending on the coefficient of friction µ

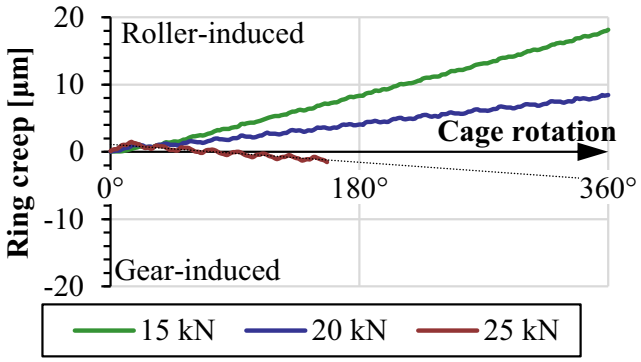


**Fig. 5** Ring creep [µm] per cage rotation depending on the normal tooth forces

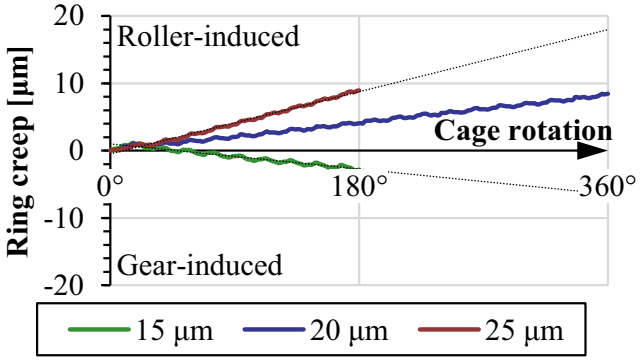


**Fig. 6** Ring creep [µm] per cage rotation depending on the interference fit

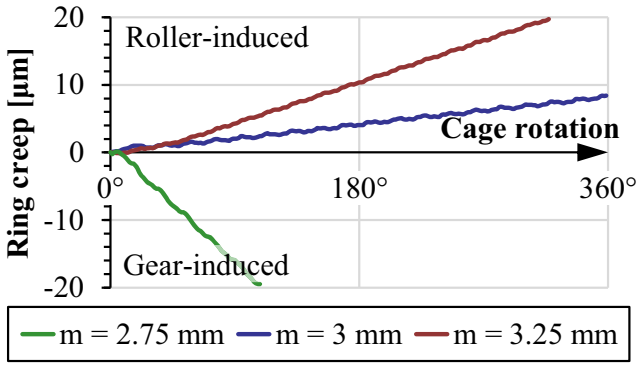


**Fig. 7** Ring creep [µm] per cage rotation depending on the teeth module m, which also changes the gear hub thickness (3.887 mm, 6.604 mm, 9.321 mm)

During the investigation, gear-induced ring creep and roller-induced ring creep, which result in a different creeping direction, must be distinguished. The Fig. 4, 5, 6, 7 show the results from the variation of coefficient of friction, normal tooth forces, interference fit as well as teeth module. The plots show the resulting ring creep, given as the induced relative movement of the outer ring relative to the planetary gear per cage rotation. This means that each roller has rotated 360° once in the bearing and the normal tooth forces has rotated around 2.48 times around the planetary gear, depending on the geometrical conditions, defined by the diameter of the outer raceway and the diameter of the rolling elements. Some of the simulations stopped early due to convergence problems, but these simulations already allow predicting a trend.

The sensitivity analysis suggests that roller-induced creep and gear-induced creep have a different dependency on all varied parameters. Consequently, this can lead to a switch of the ring creep direction. The reference simulation showed slight roller-induced ring creep. An increase of the module, the friction coefficient and the interference fit increased the roller-induced ring creep, while a decrease of these parameters led to an increase of the gear-induced ring creep and could even led to a switch of the creep direction. In contrast to this, an increase of the normal tooth forces led to more gear-induced ring creep and finally could led to a switch of creep direction. The results of these four parameters on a small bearing size are consistent with the state of the art [8], which makes the modeling approach seem reasonable.

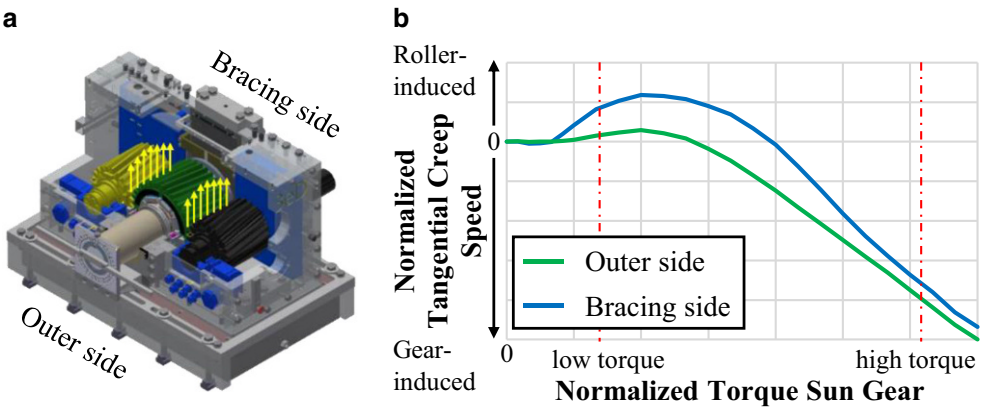


**Fig. 8** Planetary bearing test ring [2] (**a**), normalized ring creep speed over torque at sun gear rotational speed 75 $min^{-1}$ (**b**) [4]

## 5 Full-scale planetary bearing

A full-scale planetary bearing of a 1 MW WT is simulated and verified with experimental data. The planetary bearing arrangement consist of two double-row cylindrical roller bearings (SL185030) and the experimental data is obtained on a planetary bearing test bench [2] (see Fig. 8) with a measurement setup, which is presented in [4]. The "outer side" bearing correlates to the rotor-sided bearing in a WT gearbox and the "bracing side" bearing to the generator-sided bearing [4]. The Fig. 8 shows the investigated normalized tangential creep speed [4], which is the gradient of the ring creep (µm) to show the behavior at different torques.

It could be observed that for different levels of sun gear torque (normal tooth forces) at a rotational speed of 75 $min^{-1}$ the roller-induced ring creep dominates for low torque and switches to gear-induced ring creep at higher torque (see Fig. 8; [4]). The ring creep simulation (first estimation of coefficient of friction $\mu = 0.2$) can predict the qualitative ring creep direction, but the quantitative ring creep does not match with the experimental data (see Fig. 9 and 10). The gradient of simulated ring creep is at low torque 3.63 times higher for the outer side and 17 times higher for the bracing side. For high torque, the gradient of ring creep is 0.64 times lower for the outer side. In addition, the bracing side bearing seems to stand still at high torque (see Fig. 10), in contrast to gear-induced ring creep in the experiments.

Knowing from the sensitivity analysis from the small bearing size that the ring creep is highly dependent on the coefficient of friction, which is hard to predict. A sensitivity analysis for the full-scale planetary bearing regarding the coefficient of friction for high torque is performed (see Fig. 11) to improve the simulative ring creep prediction. For a coefficient of friction of 0.18, the gradient of simulated ring creep is 0.39 times lower and for a coefficient of friction of 0.22, the gradient is 0.92 times lower for the outer side.

Thus, for the outer side bearing at high torque the ring creep (gradient) matches with a coefficient of friction $\mu = 0.22$. In addition, the bracing side bearing is now clearly

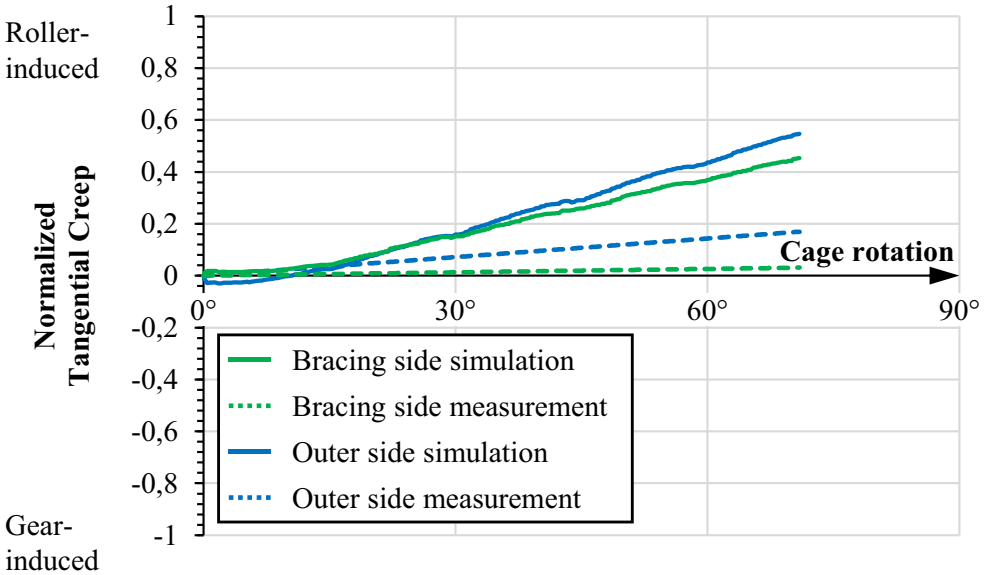


**Fig. 9** Ring creep per cage rotation at low torque (simulations with a coefficient of friction of $\mu = 0.2$)

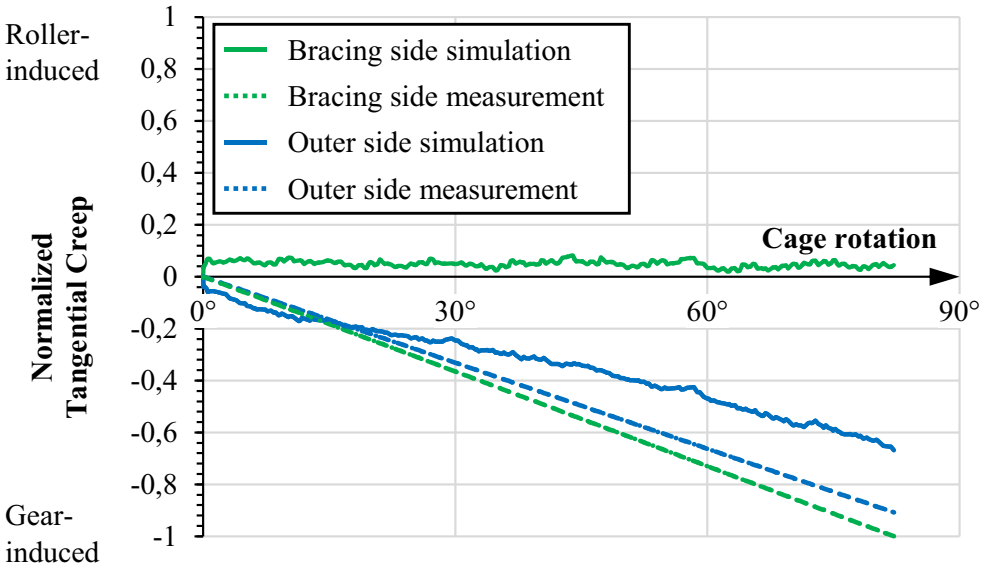


**Fig. 10** Ring creep per cage rotation at high torque (simulations with a coefficient of friction of μ = 0.2)

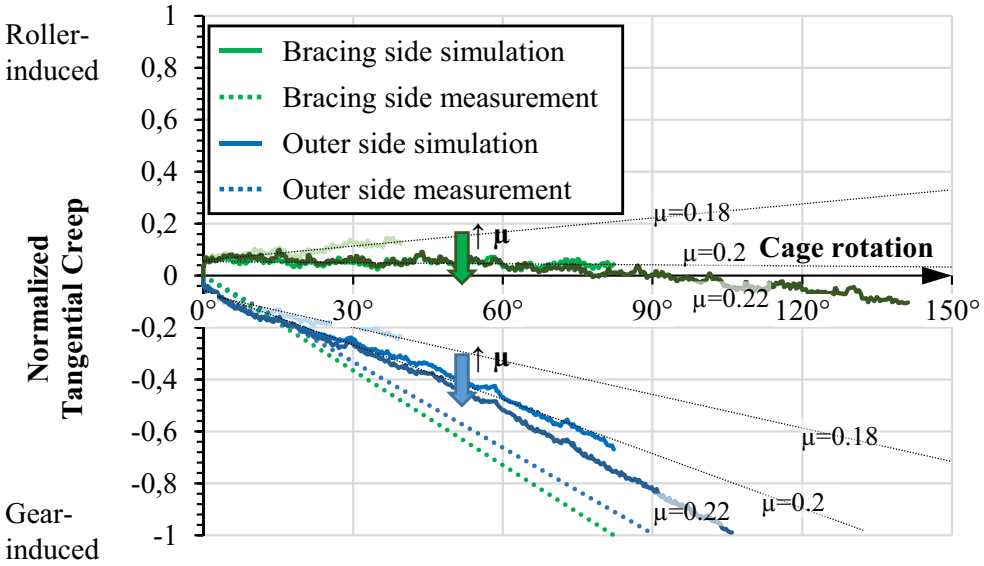


**Fig. 11** Sensitivity analysis: Ring creep [μm] per cage rotation depending on the coefficient of friction μ 0.18; 0.2; 0.22

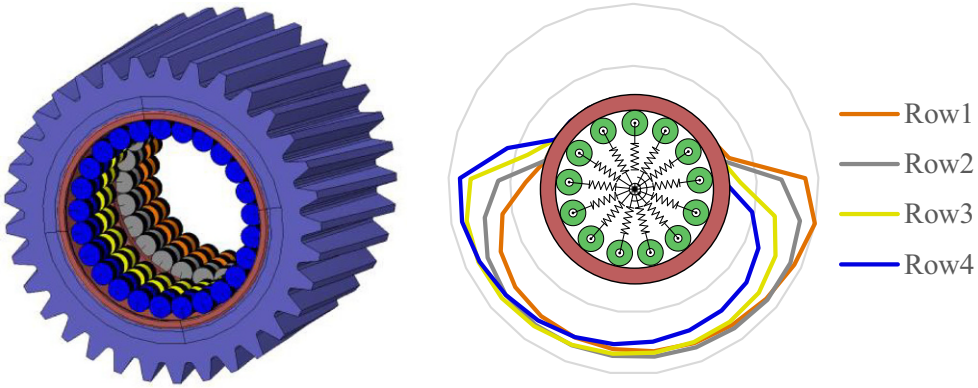


**Fig. 12** Planetary bearing load distribution per row of rollers

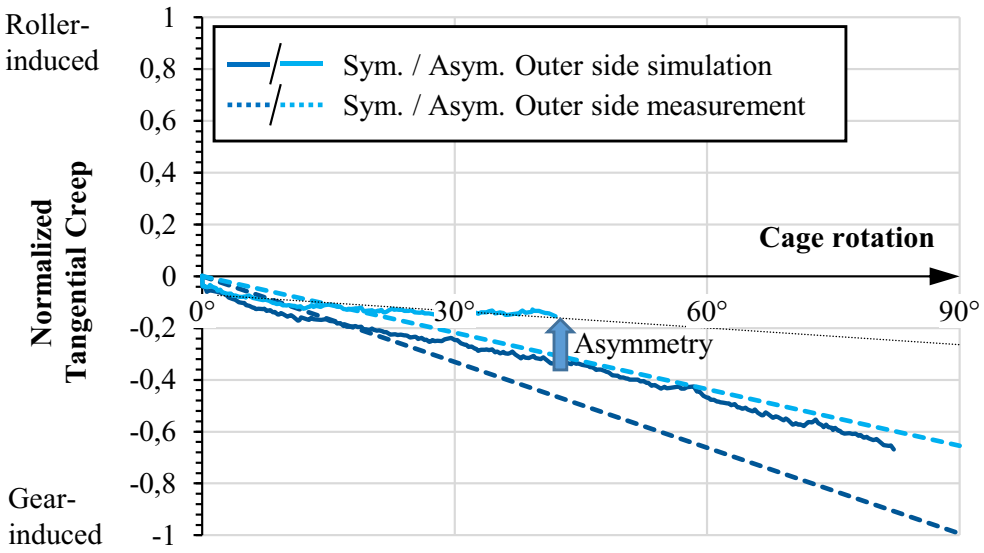


**Fig. 13** Ring creep at high torque for a symmetric and asymmetric gear load distribution (simulations with a coefficient of friction of μ = 0.2)

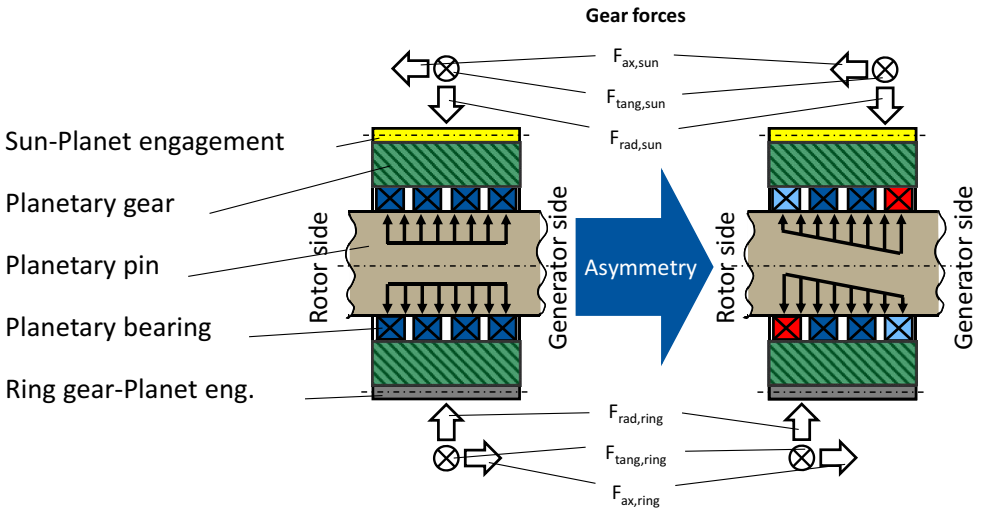


**Fig. 14** Asymmetric gear load distribution of the tooth contact: load distribution at sun-planet engagement is shifted to the bracing side (generator side) and ring gear-planet engagement to the outer side (rotor side); after [10]

subject to gear-induced ring creep but the quantitative ring creep still deviates significantly. This indicates that the model must be further optimized for the quantitative prediction of ring creep. One approach could be to include the elasticity of the pin, which normally tilts and bends under torque load [2]. The missing elasticity of the planetary pin can be also observed in the bearing load distribution (see Fig. 12); because the middle rows of the bearing arrangement should be relieved in comparison to the outer rows of the bearing arrangement, due to the bending of the planetary pin [3]. Further studies should investigate; weather the elasticity of the planetary pin can explain the deviation, by including the planetary pin elasticity into the springs, which already replicate the elasticity of the rolling element and the bearing inner ring.

Furthermore, experiments on the planetary bearing test bench [2] with non-uniform gear load distribution, which are possible due to a special adjustment kinematic to variate gear load distribution [3] show that an asymmetric gear load profile can be used to actively reduce ring creep [10]. Fig. 13 shows the ring creep for a uniform load distribution and a non-uniform gear load distribution. In this case, the gear load distribution of the tooth contact between planetary gear and sun gear is shifted to the bracing side (generator side) and vice versa the gear load distribution on the tooth contact between planetary gear and "ring gear" to the outer side (rotor side), see Fig. 14.

It can be shown (Fig. 14), that such an asymmetric gear load profile reduces for higher torque the gear-induced dominated ring creep on the outer side, which can be explained by higher roller-induced ring creep. Overall, the simulation can predict this increase in roller-induced ring creep on the outer side very well, whereas the initial offset remains. The bracing side is not considered, because of the significant deviation of the quantitative ring creep, probably due to the missing elasticity of the planetary pin.

The full-scale planetary bearing simulations can reproduce the experimental proven tendency that higher torque leads to gear-induced ring creep as well as the tendency that asymmetric gear load distribution can be used to reduce the ring creep. However, the model does not provide a good estimation of the quantitative ring creep. In all simulations, too little gear-induced ring creep was obtained and in some simulations, one of the bearing rings stood still, in contrast to the tests. By adjusting the model, e.g. by increasing the coefficient of friction and implementing the elasticity of the planetary pin, these deviations could be corrected so that the simulation results also correspond quantitatively to the test results.

## 6 Conclusion

In the presented work, a sensitivity analysis was carried out on a small bearing size (NU205) to characterize relevant influence parameters for ring creep (considered parameters are teeth module, coefficient of friction, interference fit and normal tooth forces). Also, a full-scale planetary bearing (SL185030) of a 1 MW WT was simulated and verified with experimental data. The results of the sensitivity analysis are consistent with the state of the art and the investigation of the full-scale WT planetary bearing shows that the qualitative ring creep direction can be predicted well. However, for quantitative prediction the model must be further optimized. Furthermore, it can be shown, that the reduction of ring creep through an asymmetric load profile on the teeth can be predicted with the help of FEM. In conclusion, it can be said that FEM is suitable to predict ring creep in full-scale WT planetary bearings as well as non-uniform load distributions.

**Acknowledgements** The authors would like to acknowledge the funding from the German Federal Ministry for Economic Affairs and Energy of the Research Project "WEA-GeR—Testzyklen zur Ermittlung der Robustheit von Getrieben für Windenergieanlagen" as well as for the funding of the Research Project "PlaBeD". The authors also thank the project partners for the provided insight and expertise, which assisted the research.

Supported by:

Federal Ministry
for Economic Affairs
and Energy

on the basis of a decision
by the German Bundestag

**Funding** This research has received funding from the German Federal Ministry for Economic Affairs and Energy for the Research Project "WEA-GeR—Testzyklen zur Ermittlung der Robustheit von Getrieben für Windenergieanlagen" as well as for the Research Project "PlaBeD".

**Funding** Open Access funding enabled and organized by Projekt DEAL.

**Conflict of interest** J. Gnauert, F. Schlüter, G. JacobsX, D. Bosse and S. Witter declare that they have no competing interests.



## References

1. Bundesministerium für Wirtschaft und Energie (2019) Energiedaten: Gesamtausgabe
2. Schlüter F et al (2017) Neuartiger Prüfstand für Planetenradlager in Getrieben von Windenergieanlagen. Ingenieurspiegel 4:29
3. Schlüter FM, Jacobs G, Vriesen J, Walter M, Bosse D (2019) Aktive mechanische Variation der Breitenlastverteilung einer WEA-Planetenradlagerung. In: Dresdner Maschinenelemente Kolloqium
4. Schlüter F, Jacobs G, Bosse D (2020) Investigation of wind turbine planetary bearing outer ring creep on a component test bench. In: International Bearing Conference, pp 129–132
5. Schlüter FM, Jacobs G, Bosse D, Brügge T, Schlegel F (2020) Correlation of planetary bearing outer ring creep and gear load distribution in a full-size wind turbine. J Phys Conf Ser 1452. https://doi.org/10.1088/1742-6596/1452/1/012062
6. FVA-Nr. 479 I: Wandernde Wälzlager Innen- und Außenringe unter verschiedenen Einsatzbedingungen, FVA-Heft Nr. 852, (2008).
7. FVA-Nr. 479 III: Ringwandern bei angestellten Lagern und Radiallagern unter kombinierten Belastungen. FVA-Heft Nr. 1097, (2014).
8. FVA-Nr. 479 VI: Untersuchungen des Wanderverhaltens von Wälzlagern in schrägverzahnten Planetenrädern. FVA-Heft Nr. 1281, (2018).
9. Maiwald A (2019) Special creeping movements of drive train components in wind power gearboxes. In: Conference for wind power drives 2019, pp 67–78
10. Schlüter F, Jacobs G, Bosse D, Schröder T (2020) Investigation of wind turbine planetary bearing outer ring creep on a component test bench. Presentation at International Bearing Conference. (will be in upcoming Bearing World Journal 2020)
11. Nagatomo T, Toth DG (2006) Investigation of the bearing damage progression starting from cone creep of railroad axle journal bearing. Railw Tech Res Inst Q Rep 47(3):119–124
12. Timken Wind energy solutions. https://www.timken.com/resources/brochure-wind-energy-solutions/. Accessed: 26.03.2021
13. FAG (2013) Wälzlagerschäden, Schadenserkennung und Begutachtung gelaufener Wälzlager. Schaeffler Technologies AG & Co. KG. https://www.schaeffler.com/remotemedien/media/_shared_media/08_media_library/01_publications/schaeffler_2/publication/downloads_18/wl_82102_2_de_de.pdf. Accessed: 26.03.2021

14. Froese M (2018) Why wind-turbine gearboxes fail to hit the 20-year mark. Windpower Engineering & Development. https://www.windpowerengineering.com/wind-turbine-gearboxes-fail-hit-20-year-mark/. Accessed: 26.03.2021
15. Hofmann M, Reichert J, Wagner R, Weidinger A (2005) Arrangement for mounting a planetary gear of a planetary gear. Patent DE102005049185B4.
16. Stadler K (2013) How black oxide-coated bearings can make an impact on cutting O&M costs for wind turbines. Evolution Technology Magazine. https://evolution.skf.com/us/how-black-oxide-coated-bearings-can-make-an-impact-on-cutting-om-costs-for-wind-turbines/. Accessed: 26.03.2021
17. Nagasoe Y, Wakui S, Maeyoshi Y (2015) Technology for prediction of housing wear due to outer ring creep under bearing load. Honda R D Tech Rev 27(2):103–110
18. Hastings M (2016) Detecting Bearing Creep To Avoid Replacing Gearbox. Brüel & Kjær Vibro GmbH. https://www.bkvibro.com/fileadmin/mediapool/Internet/Case_Stories/Detecting_bearing_creep_to_avoid_replacing_gearbox.pdf. Accessed: 26.03.2021